

CP-Violating 2HDMs Emerging from 3-3-1 Models

Zhiyi Fan^{1,*} and Kei Yagyu^{1,†}

¹*Department of Physics, Osaka University, Toyonaka, Osaka 560-0043, Japan*

We investigate CP violating 2 Higgs doublet models as an effective theory emerging from models with an $SU(3)_L \otimes U(1)_X$ gauge symmetry. Because of the extension of the electroweak symmetry, a characteristic structure of Yukawa interactions appears with new CP violating phases at the electroweak scale. In this scenario, the charged Higgs boson loop provides dominant and sizable contributions to the neutron electric dipole moment (nEDM) at one-loop level. We find that the prediction of the nEDM can be slightly smaller than the current upper limit, $\mathcal{O}(10^{-26}) e \text{ cm}$, with the mass of the charged Higgs boson and new CP violating phases to be a few hundred GeV and $\mathcal{O}(1)$, respectively, under the constraints from the B^0 - \bar{B}^0 mixing and the $B \rightarrow X_s \gamma$ decay.

arXiv:2201.11277v1 [hep-ph] 27 Jan 2022

* fzy1136387253@gmail.com

† yagyu@het.phys.sci.osaka-u.ac.jp

I. INTRODUCTION

The three-generation structure of matter fields assumed in the standard model (SM) has been established by the discovery of top quarks at Tevatron [1, 2]. In addition, its consistency has precisely been tested by various experiments such as B factories [3] for the quark sector and LEP for the lepton sector [4]. Furthermore, CP violation (CPV) is naturally induced from the phase of the Cabibbo-Kobayashi-Maskawa (CKM) matrix, which is required to generate non-zero baryon asymmetry of the Universe. In spite of such phenomenological successes, there is no theoretical basis for the existence of the three generations in the SM, and it has been well known that the amount of CPV from the CKM matrix is not sufficient to explain the observed baryon asymmetry [5]. These problems are expected to be solved in new physics scenarios beyond the SM.

Models with an extended electroweak (EW) gauge symmetry $SU(3)_C \otimes SU(3)_L \otimes U(1)_X$, the so-called 3-3-1 models [6–8], can simultaneously explain the origin of three generations and additional sources of CPV. The former is deduced from the condition for the gauge anomaly cancellation, by which the number of generations has to be proportional to the color degrees of freedom [8]. The extension of the EW symmetry naturally requires an extension of the Higgs sector, minimally containing three $SU(3)_L$ triplet Higgs fields, in order to realize the spontaneous symmetry breaking $SU(3)_L \otimes U(1)_X \rightarrow U(1)_{\text{em}}$ and make all charged fermions massive. Such an extended Higgs sector leads to a richer structure of Yukawa interactions and the Higgs potential with additional sources of CPV.

In this paper, we discuss an effective theory described by the $SU(2)_L \otimes U(1)_Y$ symmetry which is deduced from various 3-3-1 models with the minimal Higgs sector. All the non-SM fermions and gauge bosons are decoupled from the theory by taking the vacuum expectation value (VEV) of $SU(3)_L \otimes U(1)_X \rightarrow SU(2)_L \otimes U(1)_Y$ to be infinity. Even in this limit, the Higgs sector can be non-minimal including two $SU(2)_L$ doublet fields, namely the effective theory corresponds to a two Higgs double model (2HDM) [9]. This 2HDM is categorized into that with a discrete Z_2 symmetry whose charge for SM quarks are flavor dependent, not the flavor universal one known as the Type-I, Type-II, Type-X and Type-Y 2HDMs [10–12]. Because of the flavor dependent structure, Higgs boson couplings with quarks include new sources of flavor violation and CPV phases other than those from the CKM matrix, which can give sizable contributions to B physics observables and electric dipole moments

(EDMs). We show that the one-loop diagram with charged Higgs boson and top quark loops can give a significant contribution to the neutron EDM (nEDM), by which a portion of the parameter space is excluded by the current measurement or explored by future experiments such as the n2EDM [13]¹. This result is quite different from that in the four types of 2HDMs mentioned above [16–18] and the so-called aligned 2HDMs [19–21], where one-loop contributions are negligibly smaller than the two-loop Barr-Zee type contributions [22] due to chiral suppressions. We also find that the new phases and the mass of the charged Higgs boson can be of order one and a few hundred GeV, respectively, under the constraints from the B^0 - \bar{B}^0 mixing, the $B \rightarrow X_s \gamma$ decay and the current EDM data.

This paper is organized as follows. In Sec. II, we classify various 3-3-1 models, and show that their effective theory can be a 2HDM. In Sec. III, we discuss new contributions to the nEDM from one-loop diagrams and two-loop Barr-Zee type diagrams. We also discuss the constraints from the B^0 - \bar{B}^0 mixing and the $B \rightarrow X_s \gamma$ decay. The numerical evaluations for the nEDM are given in Sec. IV under the constraint from the B physics observables. Conclusions are given in Sec. V. In Appendix A, we present formulae for the masses of Higgs bosons and those at the large VEV limit. In Appendix B, details of the other 3-3-1 models are presented.

II. MODELS

In this section, we first classify 3-3-1 models by the difference of the definition of the electric charge Q . We then show that their effective theory corresponds to a 2HDM.

A. Classification of 3-3-1 models

Without loss of generality, Q is defined as

$$Q \equiv T_3 + Y, \quad \text{with } Y \equiv \zeta T_8 + X, \quad (1)$$

where T_3 and T_8 are the diagonal Gell-Mann matrices:

$$T_3 = \frac{1}{2} \text{diag}(1, -1, 0), \quad T_8 = \frac{1}{2\sqrt{3}} \text{diag}(1, 1, -2). \quad (2)$$

¹ CPV effects on EDMs in 3-3-1 models have also been discussed in Refs. [14, 15], in which effects of extra fermions and gauge bosons are kept by taking their masses to be of order 1 TeV.

As shown in Eq. (1), the hypercharge Y is given as the linear combination of T_8 and X with X being the $U(1)_X$ charge. In order to make Y a rational number, the ζ parameter should be proportional to $1/\sqrt{3}$. We thus express $\zeta = n/\sqrt{3}$ with n being an integer. The electric charge for $SU(3)_L$ triplets $\mathbf{3}$ is then expressed as

$$Q(\mathbf{3}) = \begin{pmatrix} \frac{1}{2} + \frac{n}{6} + X \\ -\frac{1}{2} + \frac{n}{6} + X \\ -\frac{n}{3} + X \end{pmatrix}. \quad (3)$$

The electric charge for the third component field Q_3 is expressed by that of the first component Q_1 as $Q_3 = Q_1 - (n+1)/2$, so that n should be an odd number to make Q_3 integer, by which we can avoid the appearance of exotic lepton fields with Q being half integer.

The magnitude of n is constrained by taking into account the relation among gauge coupling constants [23]. Suppose that the $SU(3)_L$ symmetry is spontaneously broken down to $SU(2)_L \otimes U(1)_Y$ by a VEV of a triplet Higgs field Φ_3 with the X charge of $n/3$, i.e., $\langle \Phi_3 \rangle = (0, 0, v_3/\sqrt{2})^T$. After the breaking of $SU(3)_L \rightarrow SU(2)_L \otimes U(1)_Y$, the 8th component of the $SU(3)_L$ gauge boson A_8^μ is mixed with the $U(1)_X$ gauge boson X^μ as

$$\begin{pmatrix} A_\mu^8 \\ X_\mu \end{pmatrix} = \begin{pmatrix} \cos \theta_{331} & \sin \theta_{331} \\ -\sin \theta_{331} & \cos \theta_{331} \end{pmatrix} \begin{pmatrix} X'_\mu \\ B_\mu \end{pmatrix}, \quad (4)$$

where B_μ (X'_μ) is the hypercharge (an additional neutral massive) gauge boson. The mixing angle θ_{331} is given by

$$\sin \theta_{331} = \frac{\zeta g_X}{\sqrt{g^2 + \zeta^2 g_X^2}}, \quad \cos \theta_{331} = \frac{g}{\sqrt{g^2 + \zeta^2 g_X^2}}. \quad (5)$$

The hypercharge coupling g_Y is given to be $g_Y = g \sin \theta_{331} = g_X \cos \theta_{331}$. Using Eq. (5), this can also be expressed as

$$\frac{1}{g_Y^2} = \frac{\zeta^2}{g^2} + \frac{1}{g_X^2}. \quad (6)$$

This relation tells us the upper limit on $|\zeta|$ which corresponds to the case with $g_X \rightarrow \infty$ as

$$\zeta^2 < \frac{g^2}{g_Y^2} = \frac{1}{\tan^2 \theta_W} \simeq (1.87)^2. \quad (7)$$

² For $n = \pm 1$, the first or second component of Φ_3 is electrically neutral, so that it can generally develop a non-zero VEV.

Therefore, possible choices for n are $n = \pm 1$ and ± 3 , i.e., $\zeta = \pm 1/\sqrt{3}$ and $\pm\sqrt{3}$.

3-3-1 models can also be classified into two categories depending on the way how three generations of left-handed quarks Q_L are embedded into the $SU(3)_L$ representation. In the first category, denoting Class-I, first two generations $Q_L^{1,2}$ are assigned to be $SU(3)_L$ anti-triplet, while the third generation Q_L^3 and three left-handed leptons are assigned to be triplet. The gauge anomaly for $[SU(3)_L]^3$ is then cancelled between six triplets from Q_L^3 and three lepton triplets and six anti-triplets from $Q_L^{1,2}$. In Class-I, we can further decompose models into those with $\zeta = -\sqrt{3}$ [24, 25], $\zeta = -1/\sqrt{3}$ [26], $\zeta = 1/\sqrt{3}$ [27, 28] and $\zeta = \sqrt{3}$ [23]. In another category, denoting Class-II, all three generations of Q_L are embedded into anti-triplets, while the lepton sector has to be extended to include nine generations of left-handed lepton triplets, the so-called E_6 inspired model [29], or to include one sextet (contributing to $[SU(3)_L]^3$ as much as the seven triplets) and two triplets, the so-called flipped model [30]. We note that in Class-II, the ζ parameter is uniquely determined to be $-1/\sqrt{3}$ for the E_6 inspired model and $1/\sqrt{3}$ for the flipped model.

In the following, we mainly focus on the Class-I model with $\zeta = -1/\sqrt{3}$ and its effective theory which is obtained by taking a large limit of the $SU(3)_L$ breaking VEV. We then comment on the models with the other ζ values and the Class-II models.

B. Model with $\zeta = -1/\sqrt{3}$

In order to discuss the effective theory of 3-3-1 models, we consider the model with $\zeta = -1/\sqrt{3}$ in Class-I as a representative one. The particle content of this model is given in Table I. In addition to the gauge symmetry, we introduce a global $U(1)'$ symmetry to avoid mixings between SM fermions and extra fermions at tree level. The scalar sector is composed of three $SU(3)_L$ triplets, which corresponds to the minimal form to break $SU(3)_L \otimes U(1)_X$ into $U(1)_{\text{em}}$ and to give all the masses of fermions except for active neutrinos ν_L^i .

The Higgs potential is generally written under the $SU(3)_L \otimes U(1)_X \otimes U(1)'$ symmetry as

$$\begin{aligned}
 V = & \sum_{i=1,3} m_i^2 |\Phi_i|^2 + \left(m_{23}^2 \Phi_2^\dagger \Phi_3 + \mu \epsilon_{ABC} \Phi_1^A \Phi_2^B \Phi_3^C + \text{h.c.} \right) \\
 & + \sum_{i=1,3} \lambda_i |\Phi_i|^4 + \sum_{i,j=1,3}^{j>i} \lambda_{ij} |\Phi_i|^2 |\Phi_j|^2 + \sum_{i,j=1,3}^{j>i} \rho_{ij} |\Phi_i^\dagger \Phi_j|^2,
 \end{aligned} \tag{8}$$

where m_{23}^2 and μ terms softly break the $U(1)'$ symmetry. By rephasing the scalar fields,

Fields	$SU(3)_C \otimes SU(3)_L \otimes U(1)_X \otimes U(1)'$	Z_2^{rem}	Components
Q_L^a	$(\mathbf{3}, \bar{\mathbf{3}}, 0, 0)$	$(+, +, -)$	$(d_L^a, -u_L^a, D_L^a)^T$
Q_L^3	$(\mathbf{3}, \mathbf{3}, +1/3, 0)$	$(+, +, -)$	$(t_L, b_L, U_L)^T$
u_R^i	$(\mathbf{3}, \mathbf{1}, +2/3, q)$	$+$	u_R^i
d_R^i	$(\mathbf{3}, \mathbf{1}, -1/3, -q)$	$+$	d_R^i
U_R	$(\mathbf{3}, \mathbf{1}, +2/3, 2q)$	$-$	U_R
D_R^a	$(\mathbf{3}, \mathbf{1}, -1/3, -2q)$	$-$	D_R^a
L_L^i	$(\mathbf{1}, \mathbf{3}, -1/3, 0)$	$(+, +, -)$	$(\nu_L^i, e_L^i, N_R^{ic})^T$
e_R^i	$(\mathbf{1}, \mathbf{1}, -1, -q)$	$+$	e_R^i
N_R^i	$(\mathbf{1}, \mathbf{1}, 0, +2q)$	$-$	N_R^i
Φ_1	$(\mathbf{1}, \mathbf{3}, +2/3, q)$	$(+, +, -)$	$(\phi_1^+, \phi_1^0, \eta_1^+)$
Φ_2	$(\mathbf{1}, \mathbf{3}, -1/3, -q)$	$(+, +, -)$	$(\phi_2^0, \phi_2^-, \eta_2^0)$
Φ_3	$(\mathbf{1}, \mathbf{3}, -1/3, -2q)$	$(-, -, +)$	$(\eta_3^0, \eta_3^-, \phi_3^0)$

TABLE I. Particle content of the model with $\zeta = -1/\sqrt{3}$, where $U(1)'$ is a softly-broken global symmetry and Z_2^{rem} is a remnant symmetry after the spontaneous breaking of $SU(3)_L \otimes U(1)_X$. The charge of Z_2^{rem} can be defined as $(-1)^{|Q'/q|+2\sqrt{3}T_8+2s}$ with s being the spin and Q' being $U(1)'$ charge. Flavor indices i and a run over 1-3 and 1-2, respectively.

all the parameters in the potential are taken to be real without loss of generality. We take $m_{23}^2 = 0$ such that the configuration of the VEVs $\langle \phi_i^0 \rangle = v_i/\sqrt{2} \neq 0$ and $\langle \eta_j^0 \rangle = 0$ is realized from the tadpole conditions, see Appendix A. In this case, the symmetry breaking is realized by the following two steps:

$$SU(3)_L \otimes U(1)_X \xrightarrow{v_3} SU(2)_L \otimes U(1)_Y \xrightarrow{v} U(1)_{\text{em}}, \quad (9)$$

where $v \equiv \sqrt{v_1^2 + v_2^2} = (\sqrt{2}G_F)^{-1/2}$ with G_F being the Fermi constant. The ratio of these VEVs is parameterized as $\tan \beta \equiv v_2/v_1$. In this configuration of the VEVs, a remnant unbroken Z_2^{rem} symmetry appears whose charges are given in Table I, by which the component fields ϕ and η do not mix with each other. In addition, the lightest neutral Z_2^{rem} -odd particle can be a candidate of dark matter.

There are 18 real scalar fields in the three triplets Φ_i , but 8 of 18 fields are absorbed into longitudinal components of the massive gauge bosons. Thus, 10 real scalar fields remain as the physical degrees of freedom. These can be classified into two pairs of singly-charged Higgs bosons (H^\pm and η^\pm), two CP-odd Higgs bosons (A, η_I) and four CP-even Higgs bosons (h, H, H_S, η_R) with h being identified with the SM-like Higgs boson. See Appendix A for

expressions of the scalar boson masses and the relation between the mass eigenbases and original ones shown in Table I.

All the Z_2^{rem} -odd scalar fields and the H_S state are decoupled by taking the $SU(3)_L$ breaking VEV v_3 to be infinity. We note that extra five gauge bosons (a pair of charged, a complex and a real neutral gauge bosons) are also decoupled by taking this limit. On the other hand, the remaining five Higgs bosons, i.e., H^\pm , A , H and h can be of order the EW scale as long as the $M^2 \equiv \mu v_3 / (\sqrt{2} \cos \beta \sin \beta)$ parameter is kept to be (EW scale)². Thus, the case with $M \sim \mathcal{O}(v)$ the Higgs sector of this model is effectively regarded as a 2HDM.

The Yukawa interaction is given by

$$\begin{aligned} \mathcal{L}_Y = & - (Y_e)_{ij} \overline{L}_L^i \Phi_1 e_R^j - (Y_N)_{ij} \overline{L}_L^i \Phi_3 N_R^j + \text{h.c.} \\ & + (Y_u^1)_{ai} \overline{Q}_L^a \Phi_1^* u_R^i - (Y_u^2)_{i\bar{a}} \overline{Q}_L^{\bar{a}} \Phi_2 u_R^i - Y_U \overline{Q}_L^3 \Phi_3 U_R + \text{h.c.} \\ & - (Y_d^1)_{i\bar{a}} \overline{Q}_L^{\bar{a}} \Phi_1 d_R^i - (Y_d^2)_{ai} \overline{Q}_L^a \Phi_2^* d_R^i - (Y_D)_{ab} \overline{Q}_L^a \Phi_3^* D_R^b + \text{h.c.} \end{aligned} \quad (10)$$

Due to the $U(1)'$ symmetry, mixings between SM fermions and extra fermions (U and D^a) do not appear. In addition, the new lepton Yukawa term $\epsilon_{ABC} (Y_L)_{ij} (\overline{L}_L^i)_A (L_L^j)_B (\Phi_1)_C$ is forbidden. We see that the extra fermion masses are given by the large VEV v_3 , while those of the SM fermions are given by the smaller VEVs v_1 and v_2 .

At the large v_3 limit, we obtain the low energy effective Lagrangian as follows:

$$\begin{aligned} \mathcal{L}_{\text{eff}} = & - (Y_e)_{ij} \ell_L^i \phi_1 e_R^j + \text{h.c.} \\ & - [(Y_u^1)_{ai} \bar{q}_L^a \tilde{\phi}_1 + (Y_u^2)_{i\bar{a}} \bar{q}_L^{\bar{a}} \phi_2] u_R^i - [(Y_d^1)_{i\bar{a}} \bar{q}_L^{\bar{a}} \phi_1 - (Y_d^2)_{ai} \bar{q}_L^a \tilde{\phi}_2] d_R^i + \text{h.c.}, \end{aligned} \quad (11)$$

where ℓ_L , q_L , ϕ_1 and ϕ_2 are the $SU(2)_L$ doublet fields defined as

$$\ell_L^i = \begin{pmatrix} \nu_L^i \\ e_L^i \end{pmatrix}, \quad q_L^i = \begin{pmatrix} u_L^i \\ d_L^i \end{pmatrix}, \quad \phi_1 = \begin{pmatrix} \phi_1^+ \\ \phi_1^0 \end{pmatrix}, \quad \phi_2 = \begin{pmatrix} \phi_2^0 \\ \phi_2^- \end{pmatrix}, \quad (12)$$

with $\tilde{\phi}_{1,2} = i\tau_2 \phi_{1,2}^*$. From Eq. (11), we see that the mass matrices for quarks are composed of two Yukawa matrices as

$$M_u = \frac{1}{\sqrt{2}} \begin{pmatrix} v_1(Y_u^1)_{11} & v_1(Y_u^1)_{12} & v_1(Y_u^1)_{13} \\ v_1(Y_u^1)_{21} & v_1(Y_u^1)_{22} & v_1(Y_u^1)_{23} \\ v_2(Y_u^2)_1 & v_2(Y_u^2)_2 & v_2(Y_u^2)_3 \end{pmatrix}, \quad M_d = \frac{1}{\sqrt{2}} \begin{pmatrix} v_2(Y_d^2)_{11} & v_2(Y_d^2)_{12} & v_2(Y_d^2)_{13} \\ v_2(Y_d^2)_{21} & v_2(Y_d^2)_{22} & v_2(Y_d^2)_{23} \\ v_1(Y_d^1)_1 & v_1(Y_d^1)_2 & v_1(Y_d^1)_3 \end{pmatrix}.$$

Therefore, after diagonalizing these mass matrices, flavor dependent structures of the quark Yukawa interactions appear. On the other hand, the mass matrix for charged leptons is

given by the single Yukawa matrix Y_e as in the SM. Performing the following bi-unitary transformations:

$$f_L = V_f f'_L, \quad f_R = U_f f'_R, \quad (f = u, d, e), \quad (13)$$

we can diagonalize these mass matrices. We then can extract the interaction terms in the mass eigenbases for fermions as follows:

$$\begin{aligned} \mathcal{L}_{\text{eff}} = & -\frac{1}{v} \bar{e}' M_e^{\text{diag}} [(s_{\beta-\alpha} - t_\beta c_{\beta-\alpha})h + (c_{\beta-\alpha} + t_\beta s_{\beta-\alpha})H + it_\beta \gamma_5 A] e' \\ & - \frac{1}{v} \sum_{\varphi=h,H,A} \sum_{q=u,d} p_\varphi^q \bar{q}' \Gamma_\varphi^q M_q^{\text{diag}} P_R q' \varphi + \text{h.c.} \\ & - \frac{\sqrt{2}}{v} [\bar{e}' M_e^{\text{diag}} t_\beta P_L \nu' + \bar{d}' (M_L P_L + M_R P_R) u'] H^- + \text{h.c.}, \end{aligned} \quad (14)$$

where $c_X = \cos X$, $s_X = \sin X$, $t_X = \tan X$, $p_h^q = p_H^q = 1$, $p_A^q = 2iI_q$ with $I_q = 1/2(-1/2)$ for $q = u(d)$ and

$$M_L = -M_d^{\text{diag}} \Gamma_A^d V_{\text{CKM}}^\dagger, \quad M_R = V_{\text{CKM}}^\dagger \Gamma_A^u M_u^{\text{diag}}. \quad (15)$$

In Eq. (14), $P_{L,R}$ are the projection operator, and $V_{\text{CKM}} \equiv V_u^\dagger V_d$ is the CKM matrix. The interaction matrices are given by

$$\begin{aligned} \Gamma_A^u &= V_u^\dagger \text{diag}(-t_\beta, -t_\beta, t_\beta^{-1}) V_u, \quad \Gamma_A^d = V_d^\dagger \text{diag}(t_\beta^{-1}, t_\beta^{-1}, -t_\beta) V_d, \\ \Gamma_H^u &= V_u^\dagger \text{diag}(c_{\beta-\alpha} + t_\beta s_{\beta-\alpha}, c_{\beta-\alpha} + t_\beta s_{\beta-\alpha}, c_{\beta-\alpha} - t_\beta^{-1} s_{\beta-\alpha}) V_u, \\ \Gamma_H^d &= V_d^\dagger \text{diag}(c_{\beta-\alpha} - t_\beta^{-1} s_{\beta-\alpha}, c_{\beta-\alpha} - t_\beta^{-1} s_{\beta-\alpha}, c_{\beta-\alpha} + t_\beta s_{\beta-\alpha}) V_d, \\ \Gamma_h^u &= V_u^\dagger \text{diag}(s_{\beta-\alpha} - t_\beta c_{\beta-\alpha}, s_{\beta-\alpha} - t_\beta c_{\beta-\alpha}, s_{\beta-\alpha} + t_\beta^{-1} c_{\beta-\alpha}) V_u, \\ \Gamma_h^d &= V_d^\dagger \text{diag}(s_{\beta-\alpha} + t_\beta^{-1} c_{\beta-\alpha}, s_{\beta-\alpha} + t_\beta^{-1} c_{\beta-\alpha}, s_{\beta-\alpha} - t_\beta c_{\beta-\alpha}) V_d. \end{aligned} \quad (16)$$

All these Γ_φ^q matrices are hermitian which turn out to be important for the discussion of the EDMs in the next section. In the 2HDMs with a softly-broken Z_2 symmetry, the diagonal matrices, e.g., $\text{diag}(-t_\beta, -t_\beta, t_\beta^{-1})$ is replace by the 3×3 identity matrix I_3 times a constant, so that the above Γ_φ^q matrices are also proportional to I_3 due to the unitarity of the V_q matrices. In the so-called alignment limit, i.e., $s_{\beta-\alpha} \rightarrow 1$, these matrices take the simple form as

$$\Gamma_H^q = -\Gamma_A^q, \quad \Gamma_h^q = 1 \quad (q = u, d). \quad (17)$$

ζ	Quarks		Leptons	Scalars		
$-1/\sqrt{3}$	$Q_{-1/3}(2)$	$Q_{2/3}(1)$	$L_0(3)$	H_S	η^0	η^\pm
$+1/\sqrt{3}$	$Q_{-1/3}(1)$	$Q_{2/3}(2)$	$L_{-1}(3)$	H_S	η^0	η^\pm
$-\sqrt{3}$	$Q_{-4/3}(2)$	$Q_{5/3}(1)$	-	H_S	η^\pm	$\eta^{\pm\pm}$
$+\sqrt{3}$	$Q_{-4/3}(1)$	$Q_{5/3}(2)$	$L_{-2}(3)$	H_S	η^\pm	$\eta^{\pm\pm}$

TABLE II. Content of heavy degrees of freedom in the Class-I models with four ζ values. The subscript for quarks (Q) and leptons (L) represents the electric charge, and the number inside parentheses denotes the number of flavors. For scalar particles, H_S represents a Z_2^{rem} -even real scalar boson, while η^0 , η^\pm and $\eta^{\pm\pm}$ are Z_2^{rem} -odd complex neutral, singly-charged and doubly-charged scalar bosons, respectively.

Thus, the Yukawa couplings for the 125 GeV Higgs boson h are the same as those of the SM values at tree level. On the other hand, the Yukawa couplings for extra Higgs bosons are non-diagonal form, because of the flavor dependent structure of the matrices $\text{diag}(-t_\beta, -t_\beta, t_\beta^{-1})$ and $\text{diag}(t_\beta^{-1}, t_\beta^{-1}, -t_\beta)$ as aforementioned.

In order to parameterize the Γ_φ^q matrices, we can express the unitary matrix V_u as follows:

$$V_u = \text{diag}(e^{i\delta_1}, e^{i\delta_2}, e^{i\delta_3}) R_{12}(\phi) R_{13}(\theta) R_{23}(\psi) \text{diag}(e^{i\delta_4}, e^{i\delta_5}, e^{i\delta_6}), \quad (18)$$

where

$$R_{12}(X) = \begin{pmatrix} c_X & -s_X & 0 \\ s_X & c_X & 0 \\ 0 & 0 & 1 \end{pmatrix}, \quad R_{13}(X) = \begin{pmatrix} c_X & 0 & -s_X \\ 0 & 1 & 0 \\ s_X & 0 & c_X \end{pmatrix}, \quad R_{23}(X) = \begin{pmatrix} 1 & 0 & 0 \\ 0 & c_X & -s_X \\ 0 & s_X & c_X \end{pmatrix}. \quad (19)$$

The unitary matrix for down-type quarks V_d is then obtained from $V_d = V_u V_{\text{CKM}}$. In this parameterization, the Γ_φ^q matrices do not depend on the $(\delta_1, \delta_2, \delta_3, \phi)$ parameters.

Before closing this section, let us comment on the other Class-I models with $\zeta = +1/\sqrt{3}$ and $\zeta = \pm\sqrt{3}$. In these models, heavy degrees of freedom, which are decoupled by taking the large v_3 limit, are different from those in the model with $\zeta = -1/\sqrt{3}$. In Table II, we show the content of extra fermions and scalar bosons decoupled from the theory. See also Appendix B for details of the particle content. The important thing here is that when we take the large v_3 limit, the effective theory of these three models is the same as that of the model with $\zeta = -1/\sqrt{3}$. For the Class-II models, however, the effective theory is different

from that discussed in this section, because all the three generations of quarks are embedded into the same $SU(3)_L$ representation, which do not lead to the flavor dependent structure as shown in Eq. (11). In addition, the lepton sector involves more complex structures including a sextet representation in the flipped model and nice triplets in the E_6 model, so that the lepton sector in their effective theory can be richer than that discussed in this section.

III. FLAVOR CONSTRAINTS

As we seen in Sec. II, 3-3-1 models introduce a 2HDM with a characteristic flavor structure in quark Yukawa interactions at the EW scale. We thus take into account flavor constraints on the parameter space, particularly those from B physics and EDMs.

A. $B^0-\bar{B}^0$ mixing

We first consider the constraint from meson mixings which happen at tree level via neutral Higgs boson exchanges, because of the flavor violating interactions given in Eq. (16). We confirm that the $B^0-\bar{B}^0$ mixing gives the most stringent constraint on the parameter space, while the others such as $D^0-\bar{D}^0$ and $K^0-\bar{K}^0$ give rather weak constraints and do not further exclude the parameter space. Therefore, we concentrate on the constraint from the $B^0-\bar{B}^0$ mixing.

According to Ref. [31], new contributions to the $B^0-\bar{B}^0$ mixing Δm_B are given by

$$\Delta m_B = \text{Re} \left[C_{LR} \left(\frac{1}{6} + \frac{m_B^2}{(m_b + m_d)^2} \right) - \frac{5}{12} (C_{LL} + C_{RR}) \frac{m_B^2}{(m_b + m_d)^2} \right] m_B f_B^2, \quad (20)$$

where m_B and f_B are the mass of the B meson and the decay constant, respectively. The coefficients C_{ij} are expressed as:

$$\begin{aligned} C_{LL} &= \sum_{\varphi=h,H,A} \frac{[p_\varphi^d m_d (\Gamma_\varphi^{d*})_{31}]^2}{m_\varphi^2 v^2}, & C_{RR} &= \sum_{\varphi=h,H,A} \frac{[p_\varphi^d m_b (\Gamma_\varphi^d)_{13}]^2}{m_\varphi^2 v^2}, \\ C_{LR} &= \sum_{\varphi=h,H,A} \frac{m_d m_b [(\Gamma_\varphi^d)_{13}]^2}{m_\varphi^2 v^2}. \end{aligned} \quad (21)$$

At the alignment limit, i.e., $s_{\beta-\alpha} = 1$, the contribution from the h mediation vanishes, because the Yukawa coupling of h takes a diagonal form. When we take $m_H = m_A$ in addition to $s_{\beta-\alpha} = 1$, C_{LL} and C_{RR} vanish, because the cancellation happens between the

contributions from the H and A mediations. In this limit, the expression for Δm_B takes a simple form as

$$\Delta m_B = m_B \frac{m_d m_b f_B^2}{m_A^2 v^2} \left[\frac{1}{3} + \frac{2m_B^2}{(m_b + m_d)^2} \right] \text{Re}[(\Gamma_A^d)_{13}]^2. \quad (22)$$

The current measured value of Δm_B is [32]

$$\Delta m_B = (3.334 \pm 0.013) \times 10^{-10} \text{ MeV}. \quad (23)$$

By comparing Eqs. (22) and (23), we can constrain $m_A (= m_H)$, t_β and the mixing/phase parameters $(\theta, \psi, \delta_{4,5,6})$. In the numerical evaluation, we simply impose that the new contribution given in Eq. (22) does not exceed the central value of the measurement.

B. $B \rightarrow X_s \gamma$

The mass of the charged Higgs boson and its Yukawa coupling are constrained by the $B \rightarrow X_s \gamma$ process. The current measured value of the branching ratio is given by [33]

$$\mathcal{B}(B \rightarrow X_s \gamma) = (3.32 \pm 0.15) \times 10^{-4}. \quad (24)$$

The bound on m_{H^\pm} has been studied in the 2HDMs with a softly-broken Z_2 symmetry at the next-to-leading order (NLO) [34–37] and at the next-to-NLO (NNLO) [38, 39] in QCD, where $m_{H^\pm} \gtrsim 600 \text{ GeV}$ has been taken in the Type-II 2HDM with $t_\beta \gtrsim 2$ [39].

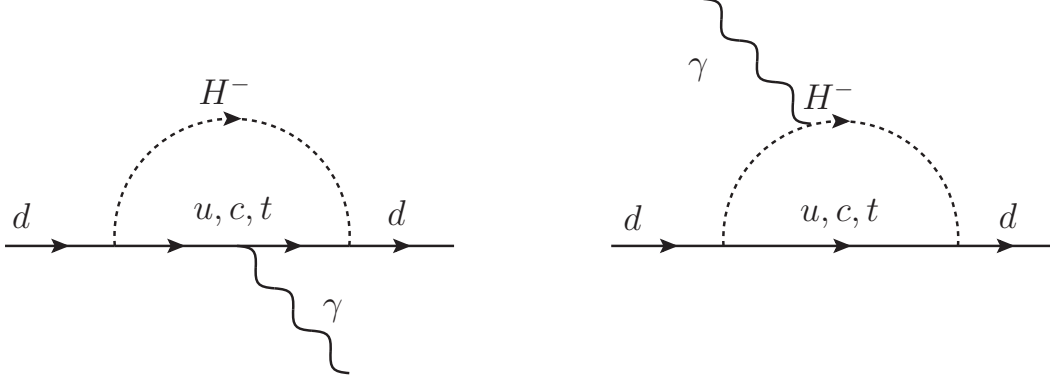
In our effective 2HDM, the situation is similar to the Type-II 2HDM if the mixing parameters θ, ψ and the phases $\delta_{4,5,6}$ are taken to be small. However, when these parameters get larger values, the constraint should be drastically different from the Type-II case. In fact, we will see in Sec. IV that the bound from the $B \rightarrow X_s \gamma$ decay tends to be relaxed when the mixing parameters are switched on.

For the numerical evaluation of the branching ratio of $B \rightarrow X_s \gamma$, we employ the expression given in Ref. [36], in which QCD and QED corrections are implemented at NLO. In Ref. [36], the branching ratio is given in terms of the X and Y parameters which are the coefficients of the Yukawa coupling for the charged Higgs boson³, and they appear as combinations of XY^* and $|Y|^2$. In our model, XY^* and $|Y|^2$ are expressed as⁴

$$XY^* = \frac{(M_L^*)_{33}(M_R)_{23}}{m_t m_b (V_{\text{CKM}})_{33}(V_{\text{CKM}}^*)_{32}}, \quad |Y|^2 = \frac{(M_R^*)_{33}(M_R)_{23}}{m_t^2 (V_{\text{CKM}})_{33}(V_{\text{CKM}}^*)_{32}}. \quad (25)$$

³ In the Type-I (Type-II) 2HDM, $X = -\cot \beta$ ($\tan \beta$) and $Y = \cot \beta$ ($\cot \beta$) [36].

⁴ We only consider the dominant top loop contribution to the decay rate.

FIG. 1. One-loop contributions to d_d .

C. Electric Dipole Moments

Generally, new CPV phases in the Yukawa interaction can induce new contributions to EDMs. Effects of CPV can be described by the following effective Lagrangian up to dimension six as

$$\begin{aligned} \mathcal{L}_{\text{eff}} = & -\frac{id_f}{2}\bar{\psi}_f\sigma^{\mu\nu}\gamma_5\psi_f F_{\mu\nu} - \frac{id_f^C}{2}\bar{\psi}_f\sigma^{\mu\nu}\gamma_5 T^A\psi_f G_{\mu\nu}^A \\ & + \frac{1}{3}C_W f_{ABC}G_{\mu\nu}^A \tilde{G}^{B\,\nu\rho}G_{\rho}^{C\,\mu} + C_{ff'}(\bar{f}f)(\bar{f}'i\gamma_5 f'). \end{aligned} \quad (26)$$

In the first line, d_f (d_f^C) denotes the coefficients of the EDM and the Chromo EDM (CEDM), where $\sigma^{\mu\nu} = \frac{i}{2}[\gamma^\mu, \gamma^\nu]$, $F_{\mu\nu}$ and $G_{\mu\nu}^A$ are the field strength tensor for the photon and gluon, respectively. In the second line, C_W ($C_{ff'}$) represents the coefficients of the Weinberg operator [40] (four-fermi interaction), where f_{ABC} is the structure constant of the $SU(3)$ group and $\tilde{G}_{\mu\nu}^A = \epsilon_{\mu\nu\rho\sigma}G^{A\rho\sigma}$.

We first consider one-loop contributions to the (C)EDM. The contributions from the neutral Higgs boson $\varphi = \{h, H, A\}$ loops are calculated to be zero shown as

$$d_q \propto \text{Im}[\Gamma_\varphi^q \Gamma_\varphi^q]_{11} = \text{Im}[(\Gamma_\varphi^q)_{1i}(\Gamma_\varphi^q)_{i1}] = \text{Im}[(\Gamma_\varphi^q)_{1i}(\Gamma_\varphi^{q*})_{1i}] = \text{Im}[|(\Gamma_\varphi^q)_{1i}|^2] = 0. \quad (27)$$

Here, we used the hermiticity of the matrices Γ_φ^q . The contribution from the charged Higgs boson loop, shown in Fig. 1, is expressed as

$$d_d^{1\text{-loop}} = \frac{em_d}{8\pi^2 v^2} \text{Im} \left[Q_u \left(V_{\text{CKM}}^\dagger \Gamma_A^u G_1^u \bar{\Gamma}_A^u V_{\text{CKM}} \right)_{11} + \left(V_{\text{CKM}}^\dagger \Gamma_A^u G_2^u \bar{\Gamma}_A^u V_{\text{CKM}} \right)_{11} \right], \quad (28)$$

$$d_u^{1\text{-loop}} = \frac{em_u}{8\pi^2 v^2} \text{Im} \left[Q_d \left(\bar{\Gamma}_A^u V_{\text{CKM}} G_1^d V_{\text{CKM}}^\dagger \Gamma_A^u \right)_{11} - \left(\bar{\Gamma}_A^u V_{\text{CKM}} G_2^d V_{\text{CKM}}^\dagger \Gamma_A^u \right)_{11} \right], \quad (29)$$

where $Q_u (Q_d) = 2/3 (-1/3)$, and we use $\Gamma_A^d = V_{\text{CKM}}^\dagger \bar{\Gamma}_A^u V_{\text{CKM}}$ with $\bar{\Gamma}_A^u \equiv \Gamma_A^u|_{\text{diag}(-t_\beta, -t_\beta, t_\beta^{-1}) \rightarrow \text{diag}(t_\beta^{-1}, t_\beta^{-1}, -t_\beta)}$. The matrices $G_{1,2}^q$ are defined as

$$G_i^u = \text{diag} \left[G_i \left(\frac{m_{H^\pm}^2}{m_u^2} \right), G_i \left(\frac{m_{H^\pm}^2}{m_c^2} \right), G_i \left(\frac{m_{H^\pm}^2}{m_t^2} \right) \right], \quad (30)$$

$$G_i^d = \text{diag} \left[G_i \left(\frac{m_{H^\pm}^2}{m_d^2} \right), G_i \left(\frac{m_{H^\pm}^2}{m_s^2} \right), G_i \left(\frac{m_{H^\pm}^2}{m_b^2} \right) \right] \quad (i = 1, 2), \quad (31)$$

with

$$G_1(x) = \frac{1 - 4x + 3x^2 - 2x^2 \ln x}{2(1-x)^3}, \quad G_2(x) = \frac{1 - x^2 + 2x \ln x}{2(1-x)^3}. \quad (32)$$

Similarly, the contribution to the CEDM is obtained by replacing the external photon with the external gluon in the left diagram of Fig. 1. We obtain

$$d_d^{C1\text{-loop}} = \frac{g_s m_d}{8\pi^2 v^2} \text{Im} \left[V_{\text{CKM}}^\dagger \Gamma_A^u G_1^u \bar{\Gamma}_A^u V_{\text{CKM}} \right]_{11}, \quad d_u^{C1\text{-loop}} = \frac{g_s m_u}{8\pi^2 v^2} \text{Im} \left[\bar{\Gamma}_A^u V_{\text{CKM}} G_1^d V_{\text{CKM}}^\dagger \Gamma_A^u \right]_{11}, \quad (33)$$

where g_s is the $SU(3)_C$ gauge coupling constant. We note that in 2HDMs with a softly-broken Z_2 symmetry, the matrices Γ_A^q are reduced to be $-t_\beta I_3$ or $t_\beta^{-1} I_3$. In this case, the above contributions are highly suppressed by the unitarity of V_{CKM} .

The magnitude of $d_d^{(C)1\text{-loop}}$ is mainly determined by the top-loop diagram, because the other contributions are suppressed by $m_q^2/m_{H^\pm}^2$ ($q \neq t$). Thus, the one-loop contribution can approximately be expressed as

$$d_d^{1\text{-loop}} \simeq \frac{e m_d}{24\pi^2 v^2} \left[2G_1 \left(\frac{m_{H^\pm}^2}{m_t^2} \right) + 3G_2 \left(\frac{m_{H^\pm}^2}{m_t^2} \right) \right] \text{Im} \left[\left(V_{\text{CKM}}^\dagger \Gamma_A^u \right)_{13} (\bar{\Gamma}_A^u V_{\text{CKM}})_{31} \right], \quad (34)$$

$$d_d^{C1\text{-loop}} \simeq \frac{g_s m_d}{8\pi^2 v^2} G_1 \left(\frac{m_{H^\pm}^2}{m_t^2} \right) \text{Im} \left[\left(V_{\text{CKM}}^\dagger \Gamma_A^u \right)_{13} (\bar{\Gamma}_A^u V_{\text{CKM}})_{31} \right]. \quad (35)$$

We note that $d_u^{(C)1\text{-loop}}$ is negligibly smaller than $d_d^{(C)1\text{-loop}}$ because of the absence of such heavy quark loops.

Second, we consider contributions from two-loop Barr-Zee type diagrams [41] to d_q . Similar to the one-loop case, diagrams with neutral Higgs boson exchanges do not contribute to the EDM, because of the hermiticity of the matrices Γ_ϕ^q . Thus, the diagram with the charged Higgs boson exchange, shown in Fig. 2, contributes to the EDM. In the alignment limit $s_{\beta-\alpha} \rightarrow 1$, the contribution from W - W - h and W - W - H loops vanishes, and the scalar-loop $d_d^{\text{BZ}}(S)$ and the fermion-loop $d_d^{\text{BZ}}(F)$ give non-zero contributions. These are calculated

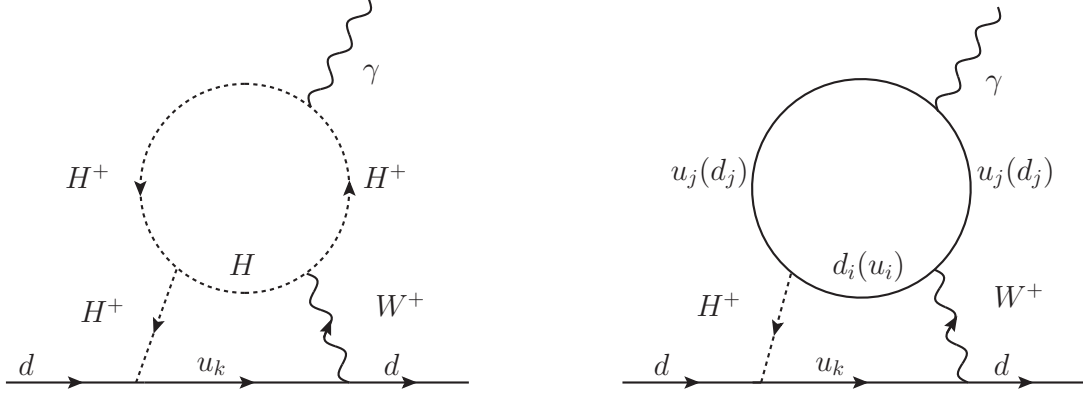


FIG. 2. Contributions to d_d from two-loop Barr-Zee type diagrams.

as

$$d_d^{\text{BZ}}(S) = - \left(\frac{1}{16\pi^2} \right)^2 \frac{eg^2}{2v} \lambda_{H^+H^-H} \sum_k \text{Im}(M_L^{1k} V_{\text{CKM}}^{k1})$$

$$\times \int_0^1 dx x \left[C_0^{\text{BZ}}(\bar{m}_{H^\pm}^2 + \tilde{m}_H^2, m_W^2, m_{H^\pm}^2) + m_{u_k}^2 D_0^{\text{BZ}}(\bar{m}_{H^\pm}^2 + \tilde{m}_H^2, m_W^2, m_{u_k}^2, m_{H^\pm}^2) \right], \quad (36)$$

$$d_d^{\text{BZ}}(F) = - \left(\frac{1}{16\pi^2} \right)^2 \frac{eg^2}{v^2} N_c \int_0^1 dx \left(Q_d + \frac{1-x}{x} Q_u \right)$$

$$\times \sum_{i,j,k} \text{Im} \left[M_L^{1k} V_{\text{CKM}}^{k1} \left(x M_L^* V_{\text{CKM}}^* M_d^{\text{diag}} + (x-2) M_R^* M_u^{\text{diag}} V_{\text{CKM}}^* \right)_{ij} \right]$$

$$\times \left[C_0^{\text{BZ}}(\bar{m}_{d_i}^2 + \tilde{m}_{u_j}^2, m_W^2, m_{H^\pm}^2) + m_{u_k}^2 D_0^{\text{BZ}}(\bar{m}_{d_i}^2 + \tilde{m}_{u_j}^2, m_W^2, m_{u_k}^2, m_{H^\pm}^2) \right], \quad (37)$$

where $\bar{m}_X^2 = m_X^2/(1-x)$, $\tilde{m}_X^2 = m_X^2/x$, and $M_{L,R}$ are given in Eq. (15). The scalar trilinear coupling $\lambda_{H^+H^-H}$ is defined by the coefficient of the vertex H^+H^-H in the Lagrangian, which is extracted to be

$$\lambda_{H^+H^-H} = \frac{2}{v} (m_H^2 - M^2) \cot 2\beta, \quad (38)$$

at the alignment limit. The loop functions C_0^{BZ} and D_0^{BZ} are given by

$$C_0^{\text{BZ}}(a, b, c) = - \frac{a \ln a}{(a-b)(a-c)} + (\text{cyclic}), \quad (39)$$

$$D_0^{\text{BZ}}(a, b, c, d) = \frac{a \ln a}{(a-b)(a-c)(a-d)} + (\text{cyclic}), \quad (40)$$

where (cyclic) denotes the other terms obtained by replacing the first term in the cyclic way,

e.g., $(a, b, c) \rightarrow (b, c, a)$. Similarly, we obtain

$$d_u^{\text{BZ}}(S) = \left(\frac{1}{16\pi^2} \right)^2 \frac{eg^2}{2v} \lambda_{H^+H^-H} \sum_k \text{Im}(V_{\text{CKM}}^{1k} M_R^{k1}) \\ \times \int_0^1 dx x [C_0^{\text{BZ}}(\bar{m}_{H^\pm}^2 + \tilde{m}_H^2, m_W^2, m_{H^\pm}^2) + m_{d_k}^2 D_0^{\text{BZ}}(\bar{m}_{H^\pm}^2 + \tilde{m}_H^2, m_W^2, m_{d_k}^2, m_{H^\pm}^2)], \quad (41)$$

$$d_u^{\text{BZ}}(F) = - \left(\frac{1}{16\pi^2} \right)^2 \frac{eg^2}{v^2} N_c \sum_{i,j,k} \int_0^1 dx \left(Q_u + \frac{x}{1-x} Q_d \right) \\ \times \sum_{i,j,k} \text{Im} \left[V_{\text{CKM}}^{1k} M_R^{k1} \left((1+x) M_L^* V_{\text{CKM}}^* M_d^{\text{diag}} - (1-x) M_R^* M_u^{\text{diag}} V_{\text{CKM}}^* \right)_{ij} \right] \\ \times \left[C_0^{\text{BZ}}(\bar{m}_{d_i}^2 + \tilde{m}_{u_j}^2, m_W^2, m_{H^\pm}^2) + m_{d_k}^2 D_0^{\text{BZ}}(\bar{m}_{d_i}^2 + \tilde{m}_{u_j}^2, m_W^2, m_{d_k}^2, m_{H^\pm}^2) \right]. \quad (42)$$

We note that the diagrams which are obtained by replacing the external photon by the gluon in Fig. 2 vanish, because the color index is not closed in the loop, so that the Barr-Zee type diagram does not contribute to d_q^C .

The nEDM d_n can be calculated by a linear combination of the EDM and CEDM by using the QCD sum rule, which are expressed as [16]

$$d_n = 0.79d_d - 0.20d_u + \frac{e}{g_s}(0.59d_d^C + 0.30d_u^C). \quad (43)$$

In our calculation, we identify $d_q = d_q^{1\text{-loop}} + d_q^{\text{BZ}}$ and $d_q^C = d_q^{C1\text{-loop}}$. The current upper limit on the nEDM d_n has been given by

$$|d_n| < 1.8 \times 10^{-26} \text{ e cm} \quad (90\% \text{ CL}), \quad (44)$$

from the nEDM experiment [42]. In future, the bound on $|d_n|$ will be improved to be $1 \times 10^{-27} \text{ e cm}$ by the n2EDM experiment with its designed performance and to be of order 10^{-28} e cm by its possible modifications [13].

We here comment on the other contributions to d_n from the Weinberg operator C_W and the four-fermi interaction C_{ff} . It has been known that the contribution from the charged Higgs boson exchange in two-loop diagrams to C_W vanishes [20, 43]. In addition, the contribution from the neutral Higgs boson exchanges to C_W in two-loop diagrams and that to C_{ff} in tree level diagrams vanish due to the hermicity of the Γ_φ^q matrices.

Let us also comment on the constraint from the electron EDM d_e whose current upper limit is given to be $|d_e| < 1.1 \times 10^{-29} \text{ e cm}$ at 90% CL at the ACME experiment [44]. The dominant contribution to d_e comes from Barr-Zee diagrams which are obtained by replacing

the external down quark d (internal up-type quarks u_k) with the electron (neutrinos) in Fig. 2. Since there is no CPV phase in the lepton Yukawa couplings for H^\pm in the limit of massless neutrinos, only the diagram with quark loops (right panel of Fig. 2) contributes to d_e . Thus, d_e can be expressed as

$$d_e \simeq - \left(\frac{1}{16\pi^2} \right)^2 \frac{eg^2 m_e}{v^2} t_\beta N_c \int_0^1 dx \left(Q_d + \frac{1-x}{x} Q_u \right) \times \sum_{i,j,k} \text{Im} \left[\left(x M_L^* V_{\text{CKM}}^* M_d^{\text{diag}} + (x-2) M_R^* M_u^{\text{diag}} V_{\text{CKM}}^* \right)_{ij} \right] C_0^{\text{BZ}}(\bar{m}_{d_i}^2 + \tilde{m}_{u_j}^2, m_W^2, m_{H^\pm}^2). \quad (45)$$

We confirm that the value of $|d_e|$ can be maximally about $7 \times 10^{-31} e \text{ cm}$ for $m_{H^\pm} = 600$ GeV and $t_\beta = 3$ by scanning the parameters $(\theta, \psi, \delta_{4,5,6})$, so that we can safely avoid the current upper limit. For $t_\beta > 10$, $|d_e|$ can exceed the upper limit, but such a large t_β value is also excluded by the constraints from d_n as well as the flavor experiments as we will see in the next section.

IV. NUMERICAL EVALUATIONS

m_c [GeV] [45]	m_t [GeV] [45]	m_d [MeV] [45]	m_b [GeV] [45]
0.901	171.7	4.22	4.2
m_B [GeV] [32]	f_B [GeV] [32]	α_{em}^{-1} [32]	
5.279	0.190	137.036	

TABLE III. SM input parameters for the calculation of the B physics constraints.

In this section, we numerically evaluate the constraint on the parameter space from the B^0 - \bar{B}^0 mixing, the $B \rightarrow X_s \gamma$ decay and the nEDM d_n discussed in Sec. III. We use the SM input parameters summarized in Tables III and IV. In Table IV, the values in the last row denote the Wolfenstein parameterization [48] of the CKM matrix:

$$V_{\text{CKM}} = \begin{pmatrix} 1 - \lambda^2/2 & \lambda & A\lambda^3(\bar{\rho} - i\bar{\eta}) \\ -\lambda & 1 - \lambda^2/2 & A\lambda^2 \\ A\lambda^3(1 - \bar{\rho} - i\bar{\eta}) & -A\lambda^2 & 1 \end{pmatrix} + \mathcal{O}(\lambda^4). \quad (46)$$

m_u [MeV] [45]	m_c [GeV] [45]	m_t [GeV] [45]	m_d [MeV] [45]	m_s [MeV] [45]	m_b [GeV] [45]
1.27	0.619	171.7	2.93	55	2.89
m_Z [GeV] [32]	m_W [GeV] [32]	α_{em}^{-1} [32]	α_s [46]		
91.1876	80.379	127.952	0.1182		
A [47]	λ [47]	$\bar{\rho}$ [47]	$\bar{\eta}$ [47]		
0.810	0.22548	0.145	0.343		

TABLE IV. SM input parameters at the m_Z scale for the calculation of the EDM constraints.

A. Case without new phases

We first discuss the case without the new CPV phases, i.e., $\delta_{4,5,6} = 0$, in which the CPV effect purely comes from the CKM phase. As we will see at the end of this subsection, the contribution from the two-loop Barr-Zee type diagrams to d_n is negligibly smaller than the one-loop contribution. Thus, we focus on the one-loop contribution.

Using the Wolfenstein parameterization given in Eq. (46), the approximate formulae for $d_d^{(C)1\text{-loop}}$ given in Eqs. (34) and (35) are expressed up to $\mathcal{O}(\lambda^5)$ as

$$\frac{d_d^{1\text{-loop}}}{e} \simeq \frac{A\bar{\eta}\lambda^3}{24\pi^2} \frac{m_d(1-t_\beta^2)}{v^2 s_\beta^2} c_\theta c_\psi \left(s_\theta - \lambda c_\theta s_\psi - \frac{\lambda^2}{2} s_\theta \right) \left[2G_1 \left(\frac{m_{H^\pm}^2}{m_t^2} \right) + 3G_2 \left(\frac{m_{H^\pm}^2}{m_t^2} \right) \right], \quad (47)$$

$$\frac{d_d^{C1\text{-loop}}}{g_s} \simeq \frac{A\bar{\eta}\lambda^3}{8\pi^2} \frac{m_d(1-t_\beta^2)}{v^2 s_\beta^2} c_\theta c_\psi \left(s_\theta - \lambda c_\theta s_\psi - \frac{\lambda^2}{2} s_\theta \right) G_1 \left(\frac{m_{H^\pm}^2}{m_t^2} \right). \quad (48)$$

As we can see that the dominant contribution is proportional to λ^3 , because one has to pick up the CPV parameter $\bar{\eta}$ in the element V_{CKM}^{13} or V_{CKM}^{31} at least once. Before numerical evaluations, let us give a few remarks on the above approximate formulae as follows:

1. For $\psi = \pi/2 + n\pi$ ($n \in \mathbb{Z}$), $d_d^{(C)1\text{-loop}}$ vanishes up to $\mathcal{O}(\lambda^5)$ as it is proportional to c_ψ . In this case, the matrices Γ_A^u and $\bar{\Gamma}_A^u$ are a block diagonal form with 2×2 and 1×1 blocks, so that the product of the combinations $(V_{\text{CKM}}^\dagger \Gamma_A^u)_{13} [= (V_{\text{CKM}}^*)_{31} (\Gamma_A^u)_{33}]$ and $(\bar{\Gamma}_A^u V_{\text{CKM}})_{31} [= (\bar{\Gamma}_A^u)_{33} (V_{\text{CKM}})_{31}]$ gives a real value at order λ^6 .
2. For $\theta = \pi/2 + n\pi$ ($n \in \mathbb{Z}$), $d_d^{(C)1\text{-loop}}$ vanishes at all orders of λ . In this case, the matrices Γ_A^u and $\bar{\Gamma}_A^u$ are diagonal forms, and the combinations $(V_{\text{CKM}}^\dagger \Gamma_A^u G_i^u \bar{\Gamma}_A^u V_{\text{CKM}})$ and $(\bar{\Gamma}_A^u V_{\text{CKM}} G_1^d V_{\text{CKM}}^\dagger \Gamma_A^u)$ appearing in Eqs. (28) and (29) are hermitian matrices.

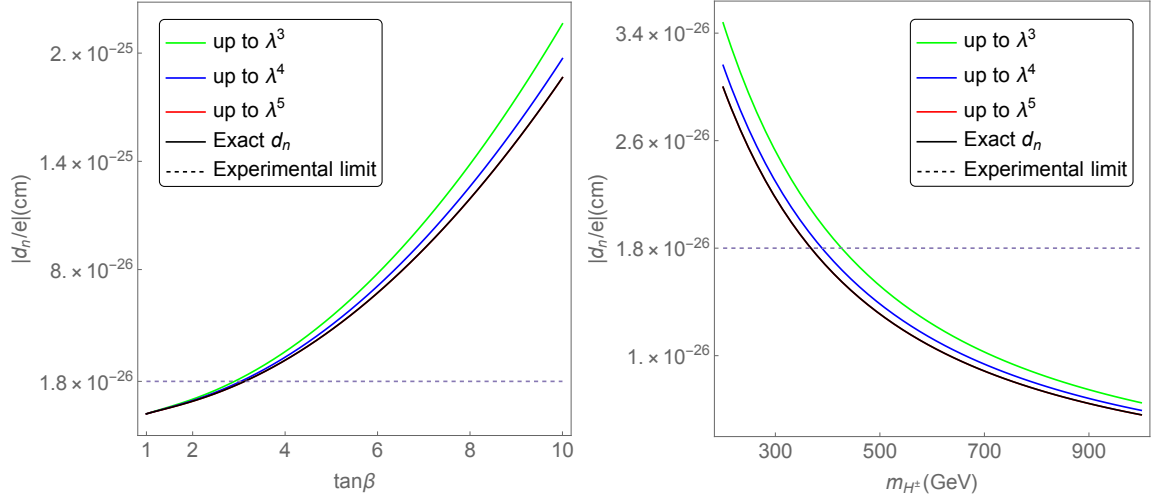


FIG. 3. Comparison of the value of $|d_n/e|$ for $\theta = \psi = \pi/3$ and $\delta_{4,5,6} = 0$ by using the approximate formulae given in Eqs. (47) and (48) up to $\mathcal{O}(\lambda^3)$, $\mathcal{O}(\lambda^4)$ and $\mathcal{O}(\lambda^5)$ and by using the exact formulae given in Eqs. (28), (29) and (33). We fix $m_{H^\pm} = 400$ GeV (left) and $\tan \beta = 3$ (right).

3. For $t_\beta = 1$, $d_d^{(C)1\text{-loop}}$ vanishes at all orders of λ . In this case, $\bar{\Gamma}_A^u = -\Gamma_A^u$ holds, so that $(V_{\text{CKM}}^\dagger \Gamma_A^u G_i^u \bar{\Gamma}_A^u V_{\text{CKM}})$ and $(\bar{\Gamma}_A^u V_{\text{CKM}} G_1^d V_{\text{CKM}}^\dagger \Gamma_A^u)$ are hermitian matrices.
4. $|d_d^{(C)1\text{-loop}}|$ is centrosymmetric about $(\theta, \psi) = (n\pi/2, m\pi)$ ($n, m \in \mathbb{Z}$) and symmetric about the lines with $\psi = \pi/2 + n\pi$ ($n \in \mathbb{Z}$).

In Fig. 3, we show the comparison of the numerical values of d_n at one-loop level by using the exact formula given in Eqs. (28), (29) and (33) and the approximate one given in Eqs. (47) and (48) as a function of t_β (left panel) and m_{H^\pm} (right panel). For the approximate formula, we use the expression up to $\mathcal{O}(\lambda^3)$, $\mathcal{O}(\lambda^4)$ and $\mathcal{O}(\lambda^5)$. We here fix the mixing angles $\theta = \psi = \pi/3$ as an example, but we confirm that the validity of the approximation is not spoiled depending on values of the mixing angles except for the case with $\psi = \pi/2 + n\pi$ ($n \in \mathbb{Z}$)⁵. It is clear that the approximation with the $\mathcal{O}(\lambda^5)$ term is quite good agreement with the exact one. In addition, we see that $|d_n|$ increases by t_β^2 for $t_\beta > 1$, and decreases by $m_t^2/m_{H^\pm}^2$ for $m_{H^\pm} \gg m_t$ as they can be read from Eqs. (47) and (48).

⁵ In this case, the approximation is no longer good, because the contribution from $\mathcal{O}(\lambda^6)$ turns out to be dominant. It, however, gives negligibly smaller values of $|d_n|$ as compared with the current upper limit, so that we do not need to care about such breakdown of the approximation.

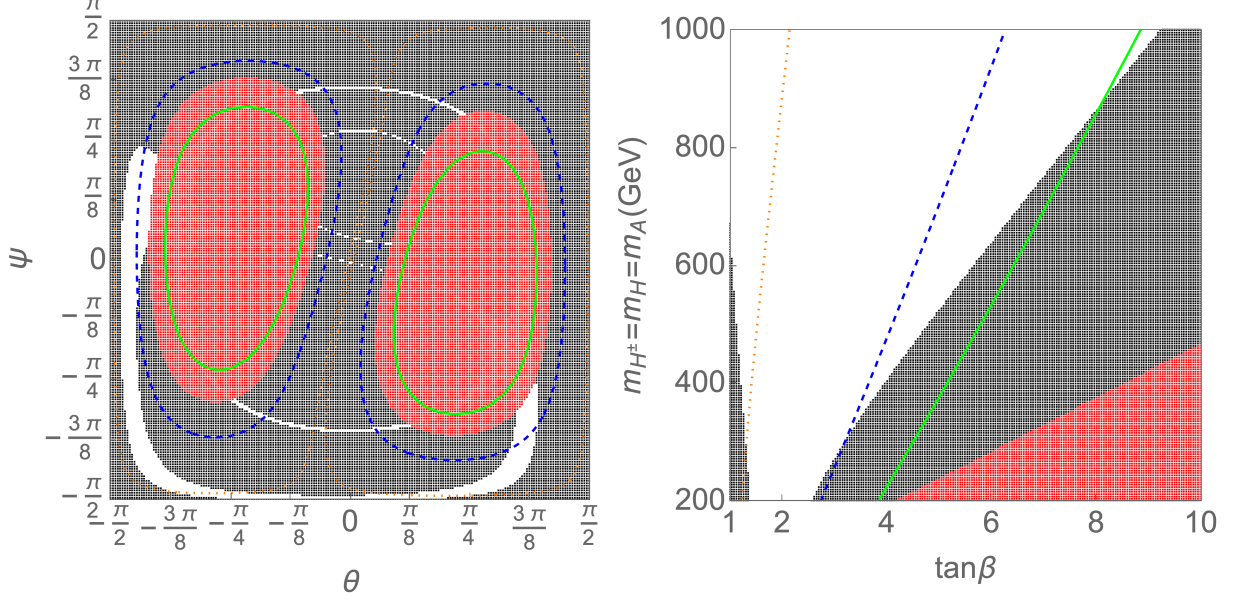


FIG. 4. Contour plots of $|d_n|$ on the θ - ψ plane with $t_\beta = 3$ and $m_{H^\pm} = 600$ GeV (left panel) and t_β - m_{H^\pm} plane with $\theta = -7\pi/16$ and $\psi = -3\pi/8$ (right panel). We take the new phases to be zero ($\delta_{4,5,6} = 0$) and degenerate masses as $m_A = m_H = m_{H^\pm}$. The regions shaded by red and black color are excluded by the constraint from B^0 - \bar{B}^0 and $B \rightarrow X_s \gamma$ data, respectively. The solid, dashed and dotted contours denote $|d_n| = 1.8 \times 10^{-26} e \text{ cm}$, 9.0×10^{-27} and $1.0 \times 10^{-27} e \text{ cm}$, respectively.

Next in Fig. 4, we show various parameter dependences, e.g., θ , ψ , t_β and m_{H^\pm} , of $|d_n|$ under the constraints from the B^0 - \bar{B}^0 and $B \rightarrow X_s \gamma$ data. We numerically find that $|d_n|$ takes a maximum value at $(\theta, \psi) \simeq (-0.79, 0.18)$, and these values almost do not depend on the choice of t_β and m_{H^\pm} , as it is expected from Eqs. (47) and (48). From the left panel of Fig. 4, we see that the region inside the green solid contour is excluded by the current nEDM data, and slightly larger regions are excluded by the B^0 - \bar{B}^0 data. We also see that the value of $|d_n|$ tends to be smaller at the corner of this plane, as it is expected from Eqs. (47) and (48). On the other hand, the exclusion by the $B \rightarrow X_s \gamma$ data shows a different pattern from that of the nEDM and the B^0 - \bar{B}^0 mixing. We find that $|d_n|$ can be of order 10^{-27} under the constraints from the flavor data, which can be explored at the n2EDM experiment. The right panel shows the constrained region on the t_β - m_{H^\pm} plane with the fixed values of the mixing angles $\theta = -7\pi/16$ and $\psi = -3\pi/8$, which are allowed by all the three constraints for $t_\beta = 3$ and $m_{H^\pm} = 600$ GeV, see the left panel. We can extract the upper limit on t_β

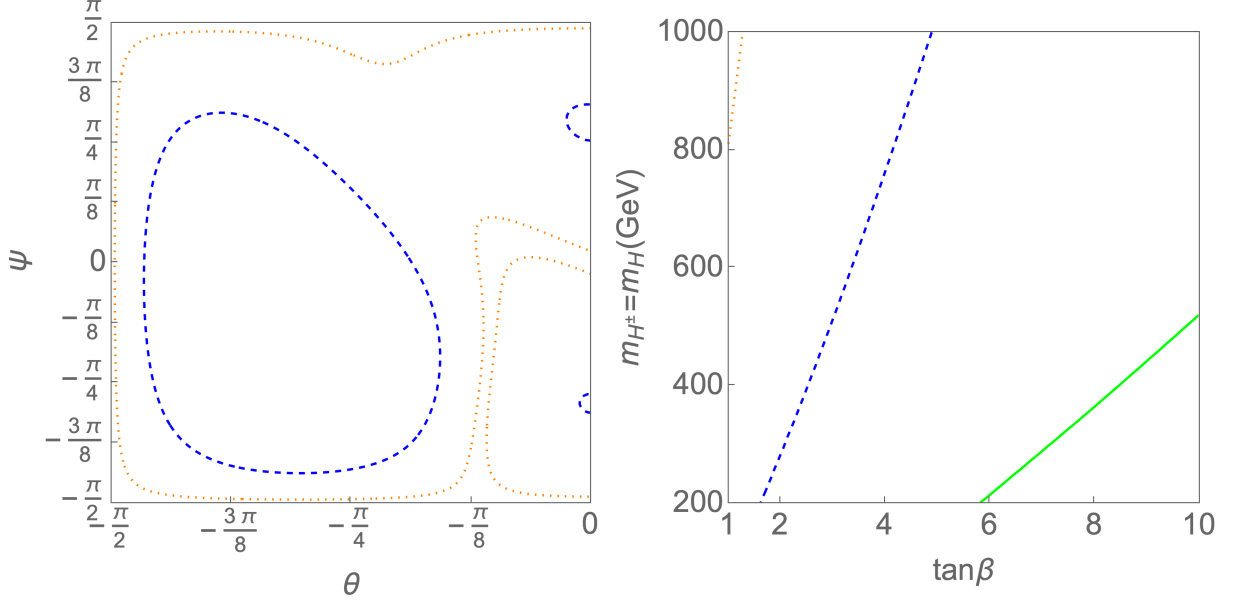


FIG. 5. Contour plots of the contribution from two-loop Barr-Zee diagrams to $|d_n|$ on the θ - ψ plane with $t_\beta = 3$ and $m_{H^\pm} = 600$ GeV (left panel) and t_β - m_{H^\pm} plane with $\theta = -7\pi/16$ and $\psi = -3\pi/8$ (right panel). We take the new phases to be zero ($\delta_{4,5,6} = 0$) and degenerate masses as $m_A = m_H = m_{H^\pm}$. The solid, dashed and dotted contours denote $|d_n| = 1.0 \times 10^{-28} e\text{cm}$, 1.0×10^{-29} and $1.0 \times 10^{-30} e\text{cm}$, respectively.

to be about 4 (8) for $m_{H^\pm} = 400$ (800) GeV from the current constraints. Remarkably, the light charged Higgs boson with a mass of order 100 GeV is allowed depending on θ , ψ and t_β by the $B \rightarrow X_s \gamma$ data. Such a light charged Higgs boson scenario has been excluded in the Type-II 2HDM.

As aforementioned, the contributions from the Barr-Zee diagram are negligibly smaller than the one-loop contribution which is shown in Fig. 4. In order to numerically show this, we exhibit the value of $|d_n|$ from the Barr-Zee diagram only in Fig. 5 with the same configuration used in Fig. 4. There are additional input parameters to evaluate the bosonic loop diagram shown in the left panel of Fig. 2, i.e., the mass of extra CP-even Higgs boson m_H and the scalar trilinear coupling $\lambda_{H^+H^-H}$. Although the dependence of those parameters on $|d_n|$ is negligibly small, we take them such that $m_H = m_{H^\pm}$ and $\lambda_{H^+H^-H} = v$ for concreteness. From Fig. 5, we see that the contribution to $|d_n|$ is typically of order 10^{-29} or smaller, which is roughly two or more than two orders of magnitude smaller than the one-loop contribution. This behavior does not significantly change for the case with non-zero phases. We thus can

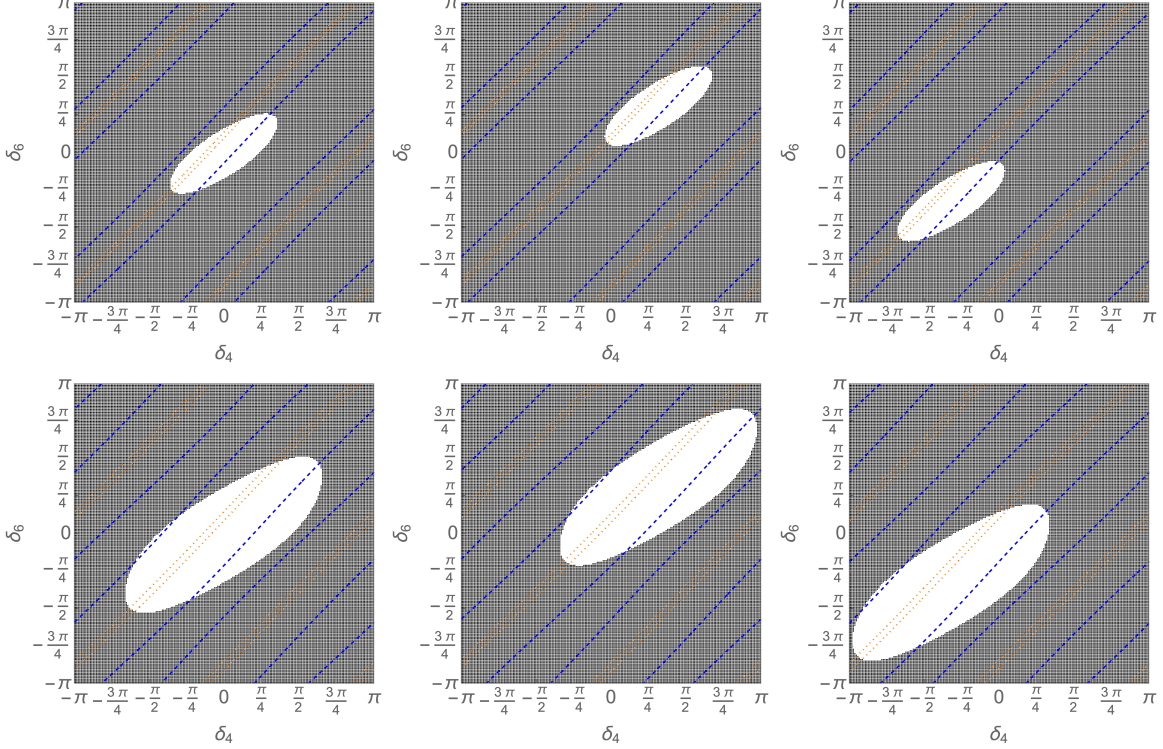


FIG. 6. Contour plots of $|d_n|$ with non-zero CPV phases $\delta_{4,5,6}$ on the δ_4 - δ_6 plane with $t_\beta = 3$, $m_H = m_A = m_{H^\pm}$, $\theta = -7\pi/16$ and $\psi = -3\pi/8$. We take $m_{H^\pm} = 400$ GeV for the upper panels and 600 GeV for the lower panels. The new phase is taken to be $\delta_5 = 0$ (left panel), $\delta_5 = 1$ (center panel) and $\delta_5 = -1$ (right panel). The regions shaded by black color are excluded by the constraint from $B \rightarrow X_s \gamma$ data. The dashed and dotted contours denote $|d_n| = 9.0 \times 10^{-27}$ and $1.0 \times 10^{-27} e \text{ cm}$, respectively.

safely neglect the Barr-Zee diagrams.

B. Non-zero phases

Finally, we discuss the case with non-zero phases $\delta_{4,5,6}$. In Fig. 6, we show the region constrained from the B^0 - \bar{B}^0 and $B \rightarrow X_s \gamma$ data and the nEDM on the δ_4 - δ_6 plane for $m_{H^\pm} = 400$ GeV (upper panels) and 600 GeV (lower panels). The other parameters are fixed as explicitly written in the caption. From the left panels ($\delta_5 = 0$), we see that at the point of the no phase limit $(\delta_4, \delta_6) = (0, 0)$, the value of $|d_n|$ is given of order 10^{-27} , while the region with $\delta_{4,6} \neq 0$ the value of $|d_n|$ can quickly glow up to 10^{-26} . We also show the similar plots for $\delta_5 = 1$ (center) and $\delta_5 = -1$ (right), where the pattern of the prediction

for $|d_n|$ is similar to the case with $\delta_5 = 0$, but the region allowed by the $B \rightarrow X_s \gamma$ data is shifted to upper and lower regions, respectively.

To conclude, we clarify that the new CPV phases $\delta_{4,5,6}$ with $\mathcal{O}(1)$ are allowed by the current B physics observables and the EDM data even for the case with a relatively light charged Higgs boson with the mass of a few hundred GeV. It should be emphasized that our scenario becomes quite similar to the Type-II 2HDM in the no-mixing limit, i.e., $\theta = \psi = 0$, so that the constraint from the $B \rightarrow X_s \gamma$ decay is severe, i.e., $m_{H^\pm} \gtrsim 600$ GeV. This, however, can drastically be changed for the case with non-zero mixing and/or non-zero additional CPV phases, where the constraint from the $B \rightarrow X_s \gamma$ decay is significantly relaxed which makes a light charged Higgs boson scenario possible. Such a scenario is also possible in the Type-I or Type-X 2HDM, but our scenario can be distinguished from them by measuring flavor violating decays of the additional Higgs bosons, e.g., $H/A \rightarrow tc$ and/or flavor dependent deviations in the h couplings from the SM predictions which do not appear in the Z_2 symmetric 2HDMs, see Ref. [9]. In addition, our scenario can be probed by future EDM experiments, e.g., n2EDM, and also can directly be tested at collider experiments by looking at decays of additional Higgs bosons, see e.g., [49] for the probe of CPV phases at electron-positron colliders.

V. CONCLUSIONS

We have discussed a CPV 2HDM emerging from 3-3-1 models at the EW scale, which are motivated to explain the three generation structure of chiral fermions. All the non-SM fermions and gauge bosons are decoupled from the theory in our approach. We have shown that various classes of 3-3-1 models having different values of the ζ parameter deduce the same structure of the 2HDM, in which flavor violating Higgs-quark couplings appear, and they contain additional CPV phases. The Yukawa couplings for quarks can be parameterized not only by $\tan \beta$ but also the mixing parameters θ, ψ and the new phases $\delta_{4,5,6}$ which arise from the bi-unitary transformation of up-type and down-type quarks. These new parameters do not appear in the softly-broken Z_2 symmetric 2HDMs, i.e., the Type-I, Type-II, Type-X and Type-Y 2HDMs, because of the flavor universal structure of the Yukawa interaction. If we take additional mixing and phase parameters to be zero, our scenario becomes Type-II 2HDM like as long as we neglect Yukawa interactions with the first and second generation

fermions.

We then have studied constraints on the parameter space from flavor observables such as the B^0 - \bar{B}^0 mixing, the $B \rightarrow X_s \gamma$ decay and the EDMs particularly for the nEDM d_n . Because of the characteristic flavor structure, the neutral Higgs bosons do not contribute to the EDMs at one-loop and two-loop Barr-Zee diagrams, and it is clarified that the dominant contribution comes from charged Higgs boson loops at one-loop level. We have found that even in the case without new phases, i.e., $\delta_{4,5,6} = 0$ the charged Higgs boson contribution to d_n can be sizable due to the CKM phase and the non-zero mixing $\theta, \psi \neq 0$. A similar region excluded by d_n can also be obtained from the B^0 - \bar{B}^0 mixing. We also have found that the constraint from the $B \rightarrow X_s \gamma$ decay can significantly be relaxed as compared with the Type-II 2HDM in the case with $\theta, \psi \neq 0$, and have shown that a light charged Higgs boson with a few hundred GeV is possible. For the case with non-zero CPV phases, i.e., $\delta_{4,5,6} \neq 0$, we see that the effect of these phases on d_n is constructive in a portion of the parameter space which are already excluded by the current measurement of d_n . On the other hand, there are regions where the new phases give a destructive effect, in which new phases of order one can be allowed under the flavor constraints. Such sizable CPV phases can be indirectly be tested at future EDM experiments such as the n2EDM experiment, and can directly be tested at collider experiments such as the high-luminosity LHC and future electron-positron colliders.

ACKNOWLEDGMENTS

The work of KY was supported in part by Grant-in-Aid for Early-Career Scientists, No. 19K14714.

Appendix A: Masses of Higgs bosons

We discuss details of the mass spectrum for scalar bosons in the model with $\zeta = -1/\sqrt{3}$ whose particle content is given in Table I.

There are five neutral components in the three Higgs triplets, which can be parameterized

as

$$\phi_i^0 = \frac{1}{\sqrt{2}}(v_i + h_i + ia_i) \quad (i = 1, 2, 3), \quad \eta_j^0 = \frac{1}{\sqrt{2}}(v'_j + \eta_j^R + i\eta_j^I) \quad (j = 2, 3). \quad (\text{A1})$$

We here introduce the VEVs for the η_j^0 fields, but either v'_2 and v'_3 can be taken to be zero by the field redefinition of Φ_2 and Φ_3 without loss of generality. We thus set $v'_2 = 0$. From the tadpole condition for η_2^R , we obtain

$$m_{23}^2 v_3 + \frac{v'_3 s_\beta}{2} \left(v v_3 \rho_{23} + \frac{v M^2}{v_3} \right) = 0. \quad (\text{A2})$$

For the case with $m_{23}^2 = 0^6$, this can be satisfied by taking $v'_3 = 0$ for arbitrary values of v and v_3 . We take this configuration throughout the paper. In this setup, the tadpole condition for η_3^R is automatically satisfied, while those for $h_{1,2,3}$ states are expressed under the assumption with $v, v_3 \neq 0$ as

$$m_1^2 - M^2 s_\beta^2 + \frac{\lambda_1}{2} v^2 c_\beta^2 + \frac{\lambda_{12}}{2} v^2 s_\beta^2 + \frac{\lambda_{13}}{2} v_3^2 = 0, \quad (\text{A3})$$

$$m_2^2 - M^2 c_\beta^2 + \frac{\lambda_{12}}{2} v^2 c_\beta^2 + \frac{\lambda_2}{2} v^2 s_\beta^2 + \frac{\lambda_{23}}{2} v_3^2 = 0, \quad (\text{A4})$$

$$m_3^2 - M^2 \frac{v^2}{v_3^2} c_\beta^2 s_\beta^2 + \frac{\lambda_{13}}{2} v^2 c_\beta^2 + \frac{\lambda_{23}}{2} v^2 s_\beta^2 + \frac{\lambda_3}{2} v_3^2 = 0, \quad (\text{A5})$$

where $M^2 \equiv \mu v_3 / (\sqrt{2} c_\beta s_\beta)$.

The mass eigenstates for the Z_2^{rem} -even scalars can be defined as

$$\begin{pmatrix} \phi_1^\pm \\ \phi_2^\pm \end{pmatrix} = R(\beta) \begin{pmatrix} G^\pm \\ H^\pm \end{pmatrix}, \quad R(x) = \begin{pmatrix} \cos x & \sin x \\ -\sin x & \cos x \end{pmatrix}. \quad (\text{A6})$$

$$\begin{pmatrix} a_1 \\ a_2 \\ a_3 \end{pmatrix} = \begin{pmatrix} -\frac{v c_\beta}{\sqrt{v_3^2 + v^2 c_\beta^2}} & -c_\beta & \frac{v_3 s_\beta}{\sqrt{v_3^2 + s_\beta^2 c_\beta^2 v^2}} \\ 0 & s_\beta & \frac{v_3 c_\beta}{\sqrt{v_3^2 + s_\beta^2 c_\beta^2 v^2}} \\ \frac{v_3}{\sqrt{v_3^2 + v^2 c_\beta^2}} & 0 & \frac{v s_\beta c_\beta}{\sqrt{v_3^2 + s_\beta^2 c_\beta^2 v^2}} \end{pmatrix} \begin{pmatrix} G_1^0 \\ G_2^0 \\ A \end{pmatrix}, \quad \begin{pmatrix} h_1 \\ h_2 \\ h_3 \end{pmatrix} = R_H \begin{pmatrix} H \\ h \\ H_S \end{pmatrix}. \quad (\text{A7})$$

where G^\pm , G_1^0 and G_2^0 are the Nambu-Goldstone (NG) bosons, and h can be identified with the discovered Higgs boson with a mass of 125 GeV. The matrix R_H is the 3×3 orthogonal matrix. We note that the eigenvectors for G_1^0 and G_2^0 , corresponding to the first and second column vectors of the 3×3 matrix in Eq. (A7), respectively, are not orthogonal, so that

⁶ This can be regarded by the choice of the soft-breaking term of the $U(1)'$ symmetry such that the subgroup \tilde{Z}_2 survives, where its charge is defined by $(-1)^{|Q'|/q}$ [50].

the orthogonal NG states are obtained by taking an appropriate basis transformation of (G_1^0, G_2^0) . The masses of physical scalar states are calculated as

$$m_{H^\pm}^2 = M^2 + \frac{\rho_{12}}{2}v^2, \quad m_A^2 = M^2 \left(1 + \frac{v^2}{v_3^2} s_\beta^2 c_\beta^2\right), \quad m_{H_i}^2 = (R_H^T M_H^2 R_H)_{ii}, \quad (\text{A8})$$

where M_H^2 is the squared mass matrix for CP-even Higgs bosons in the basis of (h_1, h_2, h_3) given as

$$M_H^2 = \begin{pmatrix} v^2 c_\beta^2 \lambda_1 + M^2 s_\beta^2 & (v^2 \lambda_{12} - M^2) s_\beta c_\beta & \frac{v}{v_3} c_\beta (v_3^2 \lambda_{13} - M^2 s_\beta^2) \\ & v^2 s_\beta^2 \lambda_2 + M^2 c_\beta^2 & \frac{v}{v_3} s_\beta (v_3^2 \lambda_{23} - M^2 c_\beta^2) \\ & & v_3^2 \lambda_3 + \frac{v^2}{v_3^2} M^2 s_\beta^2 c_\beta^2 \end{pmatrix}. \quad (\text{A9})$$

For the Z_2^{rem} -odd fields, the mass eigenstates are defined as follows:

$$\begin{pmatrix} \eta_3^\pm \\ \eta_1^\pm \end{pmatrix} = R(\gamma) \begin{pmatrix} G_\eta^\pm \\ \eta^\pm \end{pmatrix}, \quad \begin{pmatrix} \eta_3^0 \\ \eta_2^0 \end{pmatrix} = R(\delta) \begin{pmatrix} G_\eta^0 \\ \eta^0 \end{pmatrix} \quad (\text{A10})$$

where G_η^\pm and G_η^0 are the NG bosons, $\tan \gamma \equiv v_1/v_3$ and $\tan \delta \equiv v_2/v_3$. The masses of these scalar bosons are given by

$$m_{\eta^\pm}^2 = \left(1 + \frac{v^2}{v_3^2} c_\beta^2\right) \left(M^2 s_\beta^2 + \frac{v_3^2}{2} \rho_{13}\right), \quad m_{\eta^0}^2 = \left(1 + \frac{v^2}{v_3^2} s_\beta^2\right) \left(M^2 c_\beta^2 + \frac{v_3^2}{2} \rho_{23}\right). \quad (\text{A11})$$

Let us take the large VEV limit, i.e., $v_3 \gg v$ with keeping the M^2 parameter to be the size of v^2 . In this case, the η^\pm and η^0 are decoupled as their masses contain the v_3^3 term. On the other hand, the matrix M_H^2 takes a block diagonal form with small corrections proportional to v^2/v_3^2 or M^2/v_3^2 as

$$M_H^2 = \begin{pmatrix} v^2 c_\beta^2 \lambda_1 + M^2 s_\beta^2 & (v^2 \lambda_{12} - M^2) s_\beta c_\beta & 0 \\ & v^2 s_\beta^2 \lambda_2 + M^2 c_\beta^2 & 0 \\ 0 & 0 & v_3^2 \lambda_3 + \frac{v^2}{v_3^2} M^2 s_\beta^2 c_\beta^2 \end{pmatrix} + \mathcal{O}\left(\frac{v^2}{v_3^2}, \frac{M^2}{v_3^2}\right). \quad (\text{A12})$$

The orthogonal matrix R_H is then approximately expressed as

$$R_H = \begin{pmatrix} \cos \alpha + \mathcal{O}(\epsilon^2) & -\sin \alpha + \mathcal{O}(\epsilon^2) & \mathcal{O}(\epsilon) \\ \sin \alpha + \mathcal{O}(\epsilon^2) & \cos \alpha + \mathcal{O}(\epsilon^2) & \mathcal{O}(\epsilon) \\ \mathcal{O}(\epsilon) & \mathcal{O}(\epsilon) & 1 + \mathcal{O}(\epsilon^2) \end{pmatrix} \quad (\text{A13})$$

with $\epsilon = v/v_3$. Neglecting the $\mathcal{O}(\epsilon)$ term, the masses of CP-even Higgs bosons are expressed as

$$m_H^2 = (M_H^{2'})_{11}c_{\beta-\alpha}^2 - 2(M_H^{2'})_{12}c_{\beta-\alpha}s_{\beta-\alpha} + (M_H^{2'})_{22}s_{\beta-\alpha}^2, \quad (\text{A14})$$

$$m_h^2 = (M_H^{2'})_{11}c_{\beta-\alpha}^2 + 2(M_H^{2'})_{12}c_{\beta-\alpha}s_{\beta-\alpha} + (M_H^{2'})_{22}s_{\beta-\alpha}^2, \quad (\text{A15})$$

$$m_{H_S}^2 = v_3^2 \lambda_3, \quad (\text{A16})$$

and the mixing angle $\beta - \alpha$ is expressed as

$$\tan 2(\beta - \alpha) = \frac{-2(M_H^{2'})_{12}}{(M_H^{2'})_{11} - (M_H^{2'})_{22}}. \quad (\text{A17})$$

In the above expressions, $M_H^{2'}$ is the 2×2 mass matrix in the basis of $(h_1, h_2)R(-\beta)$:

$$(M_H^{2'})_{11} = v^2 (\lambda_1 c_\beta^4 + 2\lambda_3 c_\beta^2 s_\beta^2 + \lambda_2 s_\beta^4), \quad (\text{A18})$$

$$(M_H^{2'})_{12} = v^2 c_\beta s_\beta (\lambda_2 s_\beta^2 - \lambda_1^2 c_\beta^2 + \lambda^3 c_{2\beta}), \quad (\text{A19})$$

$$(M_H^{2'})_{22} = M^2 + c_\beta^2 s_\beta^2 v^2 (\lambda_1 + \lambda_2 - 2\lambda_3). \quad (\text{A20})$$

We see that at the large v_3 limit, the particle content of the Higgs sector coincides with that of the 2HDM, i.e., H^\pm , A , H and h .

Appendix B: Other Class-I models

The particle content of the other Class-I models with $\zeta = +1/\sqrt{3}$, $-\sqrt{3}$ and $+\sqrt{3}$ are shown in Tables V, VI and VII, respectively. The indices i and a run over 1-3 and 1-2, respectively. For the models with $\zeta = \pm\sqrt{3}$, we do not need to impose the $U(1)'$ symmetry, because all the extra fermions have different electric charges from that of SM fermions, and thus there is no mixing among SM and extra fermions. In the model with $\zeta = -\sqrt{3}$, the remnant Z_2^{rem} symmetry does not appear, because the SM right-handed charged leptons are embedded into the third component of the lepton triplet. In other words, the anti-symmetric Yukawa interaction $\bar{L}_L^c L_L \Phi_1$ breaks the remnant symmetry, by which η particles can decay into SM particles. On the other hand, in the model with $\zeta = +\sqrt{3}$, the remnant Z_2^{rem} symmetry appears, and its charges can be extracted from interaction terms of component fields, which are shown in Table VII. However, it has to be explicitly broken, because there is no neutral Z_2^{rem} -odd particle, i.e., it gives rise to a stable charged particle which has

Fields	$SU(3)_C \otimes SU(3)_L \otimes U(1)_X \otimes U(1)'$	Z_2^{rem}	Components
Q_L^a	$(\mathbf{3}, \bar{\mathbf{3}}, 1/3, 0)$	$(+, +, -)$	$(d_L^a, -u_L^a, U_L^a)^T$
Q_L^3	$(\mathbf{3}, \mathbf{3}, 0, 0)$	$(+, +, -)$	$(t_L, b_L, D_L)^T$
u_R^i	$(\mathbf{3}, \mathbf{1}, +2/3, q)$	$+$	u_R^i
d_R^i	$(\mathbf{3}, \mathbf{1}, -1/3, -q)$	$+$	d_R^i
U_R^a	$(\mathbf{3}, \mathbf{1}, +2/3, -2q)$	$-$	U_R^a
D_R	$(\mathbf{3}, \mathbf{1}, -1/3, 2q)$	$-$	D_R
L_L^i	$(\mathbf{1}, \mathbf{3}, -2/3, 0)$	$(+, +, -)$	$(\nu_L^i, e_L^i, E_L^i)^T$
e_R^i	$(\mathbf{1}, \mathbf{1}, -1, -q)$	$+$	e_R^i
E_R^i	$(\mathbf{1}, \mathbf{1}, -1, 2q)$	$-$	E_R^i
Φ_1	$(\mathbf{1}, \mathbf{3}, -2/3, -q)$	$(+, +, -)$	$(\phi_1^0, \phi_1^-, \eta_1^-)$
Φ_2	$(\mathbf{1}, \mathbf{3}, +1/3, q)$	$(+, +, -)$	$(\phi_2^+, \phi_2^0, \eta_2^0)$
Φ_3	$(\mathbf{1}, \mathbf{3}, +1/3, -2q)$	$(-, -, +)$	$(\eta_3^+, \eta_3^0, \phi_3^0)$

TABLE V. Particle content of the model with $\zeta = +1/\sqrt{3}$, where E^i are the extra lepton with the electric charge of -1 .

Fields	$SU(3)_c \otimes SU(3)_L \otimes U(1)_X$	Z_2^{rem}	Components
Q_L^a	$(\mathbf{3}, \bar{\mathbf{3}}, -1/3)$	$(+, +, -)$	$(d_L^a, -u_L^a, J_L^a)^T$
Q_L^3	$(\mathbf{3}, \mathbf{3}, +2/3)$	$(+, +, -)$	$(t_L, b_L, K_L)^T$
u_R^i	$(\mathbf{3}, \mathbf{1}, +2/3)$	$+$	u_R^i
d_R^i	$(\mathbf{3}, \mathbf{1}, -1/3)$	$+$	d_R^i
K_R	$(\mathbf{3}, \mathbf{1}, +5/3)$	$-$	K_R
J_R^a	$(\mathbf{3}, \mathbf{1}, -4/3)$	$-$	J_R^a
L_L^i	$(\mathbf{1}, \mathbf{3}, 0)$	$(+, +, -)$	$(\nu_L^i, e_L^i, (e_R^i)^c)^T$
Φ_1	$(\mathbf{1}, \mathbf{3}, 0)$	$(+, +, -)$	$(\phi_1^0, \phi_1^-, \eta_1^+)$
Φ_2	$(\mathbf{1}, \mathbf{3}, 1)$	$(+, +, -)$	$(\phi_2^+, \phi_2^0, \eta_2^{++})$
Φ_3	$(\mathbf{1}, \mathbf{3}, -1)$	$(-, -, +)$	$(\eta_3^-, \eta_3^{--}, \phi_3^0)$

TABLE VI. Particle content for the model with $\zeta = -\sqrt{3}$, where J^a and K are exotic quarks with the electric charge of $-4/3$ and $+5/3$, respectively.

been excluded by cosmological observations. A simple way to break the Z_2^{rem} symmetry is to introduce doubly-charged singlet scalars $S^{++} \sim (\mathbf{1}, \mathbf{1}, -2)$, by which $\Phi_3^\dagger \Phi_1 S^{++}$ and $\overline{e_R^c} e_R S^{++}$ terms can be constructed, and these allow Z_2^{rem} -odd particles to decay into SM

Fields	$SU(3)_c \otimes SU(3)_L \otimes U(1)_X$	Z_2^{rem}	Components
Q_L^a	$(\mathbf{3}, \bar{\mathbf{3}}, 2/3)$	$(+, +, -)$	$(d_L^a, -u_L^a, K_L^a)^T$
Q_L^3	$(\mathbf{3}, \mathbf{3}, -1/3)$	$(+, +, -)$	$(t_L, b_L, J_L)^T$
u_R^i	$(\mathbf{3}, \mathbf{1}, +2/3)$	$+$	u_R^i
d_R^i	$(\mathbf{3}, \mathbf{1}, -1/3)$	$+$	d_R^i
K_R	$(\mathbf{3}, \mathbf{1}, +5/3)$	$-$	K_R^a
J_R^a	$(\mathbf{3}, \mathbf{1}, -4/3)$	$-$	J_R
L_L^i	$(\mathbf{1}, \mathbf{3}, -1)$	$(+, +, -)$	$(\nu_L^i, e_L^i, F_L^i)^T$
e_R^i	$(\mathbf{1}, \mathbf{1}, -1)$	$+$	e_R^i
F_R^i	$(\mathbf{1}, \mathbf{1}, -2)$	$-$	F_R^i
Φ_1	$(\mathbf{1}, \mathbf{3}, -1)$	$(+, +, -)$	$(\phi_1^0, \phi_1^-, \eta_1^{--})$
Φ_2	$(\mathbf{1}, \mathbf{3}, 0)$	$(+, +, -)$	$(\phi_2^+, \phi_2^0, \eta_2^-)$
Φ_3	$(\mathbf{1}, \mathbf{3}, 1)$	$(-, -, +)$	$(\eta_3^{++}, \eta_3^+, \phi_3^0)$

TABLE VII. Particle content for the model with $\zeta = +\sqrt{3}$, where J and K (F) are exotic quarks (leptons) with the electric charge of $-4/3$ and $+5/3$ (-2), respectively.

particles.

-
- [1] F. Abe *et al.* (CDF), Phys. Rev. Lett. **74**, 2626 (1995), arXiv:hep-ex/9503002.
 - [2] S. Abachi *et al.* (D0), Phys. Rev. Lett. **74**, 2632 (1995), arXiv:hep-ex/9503003.
 - [3] A. J. Bevan *et al.* (BaBar, Belle), Eur. Phys. J. C **74**, 3026 (2014), arXiv:1406.6311 [hep-ex].
 - [4] S. Schael *et al.* (ALEPH, DELPHI, L3, OPAL, SLD, LEP Electroweak Working Group, SLD Electroweak Group, SLD Heavy Flavour Group), Phys. Rept. **427**, 257 (2006), arXiv:hep-ex/0509008.
 - [5] P. Huet and E. Sather, Phys. Rev. D **51**, 379 (1995), arXiv:hep-ph/9404302.
 - [6] M. Singer, J. W. F. Valle, and J. Schechter, Phys. Rev. **D22**, 738 (1980).
 - [7] J. W. F. Valle and M. Singer, *11th International Symposium on Lepton and Photon Interactions at High Energies Ithaca, New York, August 4-9, 1983*, Phys. Rev. **D28**, 540 (1983).
 - [8] P. H. Frampton, Phys. Rev. Lett. **69**, 2889 (1992).
 - [9] H. Okada, N. Okada, Y. Orikasa, and K. Yagyu, Phys. Rev. D **94**, 015002 (2016), arXiv:1604.01948 [hep-ph].

- [10] Y. Grossman, Nucl. Phys. **B426**, 355 (1994), arXiv:hep-ph/9401311 [hep-ph].
- [11] V. Barger, H. E. Logan, and G. Shaughnessy, Phys. Rev. D **79**, 115018 (2009), arXiv:0902.0170 [hep-ph].
- [12] M. Aoki, S. Kanemura, K. Tsumura, and K. Yagyu, Phys. Rev. **D80**, 015017 (2009), arXiv:0902.4665 [hep-ph].
- [13] N. J. Ayres *et al.* (n2EDM), Eur. Phys. J. C **81**, 512 (2021), arXiv:2101.08730 [physics.ins-det].
- [14] G. De Conto and V. Pleitez, Phys. Rev. D **91**, 015006 (2015), arXiv:1408.6551 [hep-ph].
- [15] G. De Conto and V. Pleitez, (2016), arXiv:1606.01747 [hep-ph].
- [16] T. Abe, J. Hisano, T. Kitahara, and K. Tobioka, JHEP **01**, 106 (2014), [Erratum: JHEP 04, 161 (2016)], arXiv:1311.4704 [hep-ph].
- [17] K. Cheung, A. Jueid, Y.-N. Mao, and S. Moretti, Phys. Rev. D **102**, 075029 (2020), arXiv:2003.04178 [hep-ph].
- [18] W. Altmannshofer, S. Gori, N. Hamer, and H. H. Patel, Phys. Rev. D **102**, 115042 (2020), arXiv:2009.01258 [hep-ph].
- [19] A. Pich and P. Tuzon, Phys. Rev. D **80**, 091702 (2009), arXiv:0908.1554 [hep-ph].
- [20] M. Jung and A. Pich, JHEP **04**, 076 (2014), arXiv:1308.6283 [hep-ph].
- [21] S. Kanemura, M. Kubota, and K. Yagyu, JHEP **08**, 026 (2020), arXiv:2004.03943 [hep-ph].
- [22] S. M. Barr and A. Zee, Phys. Rev. Lett. **65**, 21 (1990), [Erratum: Phys.Rev.Lett. 65, 2920 (1990)].
- [23] R. M. Fonseca and M. Hirsch, Phys. Rev. D **94**, 115003 (2016), arXiv:1607.06328 [hep-ph].
- [24] P. H. Frampton, Physical Review Letters **69**, 2889 (1992).
- [25] F. Pisano and V. Pleitez, Physical Review D **46**, 410 (1992).
- [26] M. Singer, Physical Review D **22**, 738 (1980).
- [27] V. Pleitez, Physical Review D **53**, 514 (1996).
- [28] M. Özer, Physical Review D **54**, 1143 (1996).
- [29] L. A. Sanchez, W. A. Ponce, and R. Martinez, Phys. Rev. D **64**, 075013 (2001), arXiv:hep-ph/0103244.
- [30] R. M. Fonseca and M. Hirsch, Journal of High Energy Physics **2016** (2016), 10.1007/jhep08(2016)003.
- [31] F. Gabbiani, E. Gabrielli, A. Masiero, and L. Silvestrini, Nucl. Phys. B **477**, 321 (1996), arXiv:hep-ph/9604387.

- [32] P. Zyla *et al.* (Particle Data Group), PTEP **2020**, 083C01 (2020).
- [33] Y. S. Amhis *et al.* (HFLAV), Eur. Phys. J. C **81**, 226 (2021), arXiv:1909.12524 [hep-ex].
- [34] M. Ciuchini, G. Degrossi, P. Gambino, and G. F. Giudice, Nucl. Phys. B **527**, 21 (1998), arXiv:hep-ph/9710335.
- [35] A. L. Kagan and M. Neubert, Eur. Phys. J. C **7**, 5 (1999), arXiv:hep-ph/9805303.
- [36] F. Borzumati and C. Greub, Phys. Rev. D **58**, 074004 (1998), arXiv:hep-ph/9802391.
- [37] F. Borzumati and C. Greub, Phys. Rev. D **59**, 057501 (1999), arXiv:hep-ph/9809438.
- [38] M. Misiak *et al.*, Phys. Rev. Lett. **98**, 022002 (2007), arXiv:hep-ph/0609232.
- [39] M. Misiak and M. Steinhauser, Eur. Phys. J. C **77**, 201 (2017), arXiv:1702.04571 [hep-ph].
- [40] S. Weinberg, Physical Review Letters **63**, 2333 (1989).
- [41] S. M. Barr, Physical Review Letters **65**, 21 (1990).
- [42] C. Abel *et al.* (nEDM), Phys. Rev. Lett. **124**, 081803 (2020), arXiv:2001.11966 [hep-ex].
- [43] H. E. Logan, S. Moretti, D. Rojas-Ciofalo, and M. Song, JHEP **07**, 158 (2021), arXiv:2012.08846 [hep-ph].
- [44] V. Andreev *et al.* (ACME), Nature **562**, 355 (2018).
- [45] Z.-z. Xing, H. Zhang, and S. Zhou, Phys. Rev. D **77**, 113016 (2008), arXiv:0712.1419 [hep-ph].
- [46] S. Aoki *et al.* (Flavour Lattice Averaging Group), Eur. Phys. J. C **80**, 113 (2020), arXiv:1902.08191 [hep-lat].
- [47] J. Charles *et al.*, Phys. Rev. D **91**, 073007 (2015), arXiv:1501.05013 [hep-ph].
- [48] P. A. Zyla *et al.* (Particle Data Group), PTEP **2020**, 083C01 (2020).
- [49] S. Kanemura, M. Kubota, and K. Yagyu, JHEP **04**, 144 (2021), arXiv:2101.03702 [hep-ph].
- [50] A. Das, K. Enomoto, S. Kanemura, and K. Yagyu, Phys. Rev. D **101**, 095007 (2020), arXiv:2003.05857 [hep-ph].